The Journal of Nutrition
Biochemical, Molecular, and Genetic Mechanisms

Dietary Methionine Restriction Regulates Liver Protein Synthesis and Gene Expression Independently of Eukaryotic Initiation Factor 2 Phosphorylation in Mice[1–3]

Ashley P Pettit,[4] William O Jonsson,[4] Albert R Bargoud,[4] Emily T Mirek,[4] Frederick F Peelor III,[5] Yongping Wang,[4] Thomas W Gettys,[6] Scot R Kimball,[7] Benjamin F Miller,[5] Karyn L Hamilton,[5] Ronald C Wek,[8] and Tracy G Anthony[4]*

[4]Department of Nutritional Sciences, Rutgers University, New Brunswick, NJ; [5]Department of Health and Exercise Science, Colorado State University, Fort Collins, CO; [6]Laboratory of Nutrient Sensing and Adipocyte Signaling, Pennington Biomedical Research Center, Baton Rouge, LA; [7]Department of Cellular and Molecular Physiology, Pennsylvania State University College of Medicine, Hershey PA; and [8]Department of Biochemistry of Molecular Biology, Indiana University School of Medicine, Indianapolis, IN

Abstract

Background: The phosphorylation of eukaryotic initiation factor 2 (p-eIF2) during dietary amino acid insufficiency reduces protein synthesis and alters gene expression via the integrated stress response (ISR).

Objective: We explored whether a Met-restricted (MR) diet activates the ISR to reduce body fat and regulate protein balance.

Methods: Male and female mice aged 3–6 mo with either whole-body deletion of general control nonderepressible 2 (*Gcn2*) or liver-specific deletion of protein kinase R-like endoplasmic reticulum kinase (*Perk*) alongside wild-type or floxed control mice were fed an obesogenic diet sufficient in Met (0.86%) or an MR (0.12% Met) diet for ≤5 wk. Ala enrichment with deuterium was measured to calculate protein synthesis rates. The guanine nucleotide exchange factor activity of eIF2B was measured alongside p-eIF2 and hepatic mRNA expression levels at 2 d and 5 wk. Metabolic phenotyping was conducted at 4 wk, and body composition was measured throughout. Results were evaluated with the use of ANOVA ($P < 0.05$).

Results: Feeding an MR diet for 2 d did not increase hepatic p-eIF2 or reduce eIF2B activity in wild-type or *Gcn2*$^{-/-}$ mice, yet many genes transcriptionally regulated by the ISR were altered in both strains in the same direction and amplitude. Feeding an MR diet for 5 wk increased p-eIF2 and reduced eIF2B activity in wild-type but not *Gcn2*$^{-/-}$ mice, yet ISR-regulated genes altered in both strains similarly. Furthermore, the MR diet reduced mixed and cytosolic but not mitochondrial protein synthesis in both the liver and skeletal muscle regardless of *Gcn2* status. Despite the similarities between strains, the MR diet did not increase energy expenditure or reduce body fat in *Gcn2*$^{-/-}$ mice. Finally, feeding the MR diet to mice with *Perk* deleted in the liver increased hepatic p-eIF2 and altered body composition similar to floxed controls.

Conclusions: Hepatic activation of the ISR resulting from an MR diet does not require p-eIF2. *Gcn2* status influences body fat loss but not protein balance when Met is restricted. *J Nutr* 2017;147:1031–40.

Keywords: ATF4, GCN2, PERK, integrated stress response, eIF2B

Introduction

Met restriction leads to physiologic responses that extend lifespans (1–4) and confer protection against metabolic diseases by reducing visceral fat (5), increasing insulin sensitivity (6), and ameliorating hepatosteatosis by altering lipid metabolism (7–9). The mechanism by which these physiologic changes occur is multifaceted and include but are not limited to sympathetic outflow, mitochondrial uncoupling, and the transcriptional control of genes such as hepatokine fibroblast growth factor 21 (FGF21)[9] (10).

Dietary amino acid insufficiency increases phosphorylation of eukaryotic initiation factor 2 (p-eIF2) via general control nonderepressible 2 (GCN2) kinase (11, 12). p-eIF2 activates the integrated stress response (ISR), a mechanism that maintains cellular homeostasis under environmental stress (13). ISR activation reduces general protein synthesis at the level of mRNA translation initiation, slowing GDP/GTP exchange on eukaryotic initiation factor 2 (eIF2) by guanine nucleotide exchange factor eIF2B (14). Reduced eIF2B activity causes ribosomes to scan through upstream initiation codons in the 5′ leader of some mRNAs, favoring the synthesis of full-length activating transcription factor 4 (ATF4) instead of translating its inhibitory upstream open-reading frames (15). ATF4 is a master regulator

Manuscript received December 21, 2016. Initial review completed January 20, 2017. Revision accepted March 15, 2017.
First published online April 26, 2017; doi:10.3945/jn.116.246710.

of metabolism that alters the expression of genes containing amino acid response elements in order to regain homeostasis and is the best characterized preferentially translated mRNA during amino acid insufficiency (16, 17). ATF4-driven changes in gene expression after protein and amino acid deficiency alter TG metabolism in part via FGF21 (18–20) and in response to sulfur amino acid deficiency regulate cellular methylation and antioxidant metabolism through the transsulfuration pathway (21–24).

The role of GCN2 in activating the ISR to Met restriction is unclear. We recently reported that feeding a Met-restricted (MR) diet activated a noncanonical protein kinase R-like endoplasmic reticulum (ER) kinase (PERK)/nuclear factor-like 2 (Nrf2) axis (25). The PERK-mediated p-eIF2 in the liver corresponded with decreased reduced glutathione (GSH) status and increased circulating FGF21 but not ER stress after 14 wk of MR feeding. Although a regulatory role for GCN2 at time points before 14 wk may exist as described with dietary protein restriction (19) and leucine deprivation (12), we have noted previously that hepatic *Fgf21* expression increased over the first 6 d of MR feeding despite any change or reduction in p-eIF2 levels. Furthermore, studies in mice have shown that blocking GSH synthesis resulted in a lean insulin-sensitive phenotype similar to Met restriction (26, 27). The combination of these observations prompted us to further investigate the relations between hepatic p-eIF2, GSH status, and the induction of the ISR by Met restriction. In this study, we hypothesized that GCN2-mediated p-eIF2 would be required for sensing Met restriction early on and that the loss of GCN2 would delay the hepatic ISR to Met restriction. To test this hypothesis, wild-type (WT) mice and C57BL/6J WT and C57BL/6J mice with *Gcn2* deleted (GC) were fed MR diets for 2 d or 5 wk. In addition, to investigate the possible impact of hepatic PERK on p-eIF2, mice with liver-specific knockouts for *Perk* were tested after 5 wk of the MR diet.

Methods

Animal protocol. All animal procedures and protocols were reviewed and approved by the Rutgers University Institutional Animal Care and Use Committee. Male and female mice were bred and maintained in a conventional animal facility. Unless otherwise noted, mice were individually housed in solid-bottom clear plastic cages containing corncob bedding and environmental enrichment. Cages were located in a humidity-controlled room on a 12-h light-dark photoperiod. Before experimental acclimation, mice had unrestricted access to water and a commercial pelleted diet (LabDiet Rodent 5001).

TABLE 1 Composition of experimental diets[1]

Macronutrient	g	kcal
Protein, %	18	14
Carbohydrates, %	35	26
Fat, %	35	60
Total, %	88	100

[1] Both the obesogenic diet and Met-restricted experimental diet were 5.3 kcal/g energy density.

Diets and experimental designs. The diets used (**Tables 1** and **2**) were based on those used to assess the ability of Met restriction in promoting leanness in mice fed an obesogenic diet (OD) (29). GC mice were acclimated to a Met-sufficient (0.86% Met) OD for ≥1 wk. After this period of acclimatization, half the WT and GC cohorts remained on the OD, whereas the other half were switched to a diet similar in carbohydrate and fat composition but restricted in Met (0.12% Met) for the remainder of the experiment. Both diets were devoid of Cys.

Expt. 1. Young adult male and female WT and GC mice aged 3–6 mo (n = 6–10 per strain and per diet, respectively) were conventionally housed as described previously and fed an OD or MR diet for 2 d or 5 wk.

Expt. 2. Young adult male WT and GC mice aged 3–6 mo (n = 4 per strain and per diet, respectively) were housed in wire-bottomed cages with environmental enrichment (polyvinyl chloride pipe providing a solid place to rest) and fed an OD or MR diet for 5 wk.

Expt. 3. Young adult male WT and GC mice aged 3–6 mo (n = 10 per strain and per diet, respectively) were conventionally housed as described previously and fed an OD or an MR diet for ≥21 d. Mice were injected with a bolus dose of 99% deuterium oxide at the start of

TABLE 2 Ingredients of experimental diets[1]

	g	kcal
L-Arg	11.2	45
L-His-HCl-H_2O	3.3	13
L-Iso	8.2	33
L-Leu	11.1	44
L-Lys	14.4	58
L-Met	8.6 (1.2)	34 (5)
L-Phe	11.6	46
L-Thr	8.2	33
L-Trp	1.8	7
L-Val	8.2	33
L-Glu	27 (34.4)	108 (138)
Gly	23.3	93
Corn starch	0	0
Maltodextrin	56.8	227
Dextrose	50	200
Sucrose	150	600
Cellulose	50	0
Lard	219	1971
Corn oil	46	414
Mineral mix S10001[2]	35	0
Vitamin mix V10001[2]	10	40
Choline bitartarate	2	0
Red #40 FD&C	0	0
Yellow #5 FD&C	0.025 (0)	0 (0)
Blue #1 FD&C	0.025 (0.05)	0 (0)
Total	755.75	4000

[1] Values shown in parentheses reflect alterations in the Met-restricted diet.
[2] As formulated previously in reference 28.

[1] Supported by NIH grants HD070487 (to TGA), DK109714 (to TGA and RCW), AG042569 (to BFM and KLH), and DK096311 (to TWG); USDA National Institute of Food and Agriculture grant NC1184 (to TGA); and INSPIRE NIH-Institutional Research and Academic Career Development Awards postdoctoral training grant K12GM093854 (to APP).
[2] Author disclosures: AP Pettit, WO Jonsson, AR Bargoud, ET Mirek, FF Peelor III, Y Wang, TW Gettys, SR Kimball, BF Miller, KL Hamilton, RC Wek, and TG Anthony, no conflicts of interest.
[3] Supplemental Figures 1 and 2 and Supplemental Tables 1–3 are available from the ''Online Supporting Material'' link in the online posting of the article and from the same link in the online table of contents at http://jn.nutrition.org.
*To whom correspondence should be addressed. E-mail: tracy.anthony@rutgers.edu.
[9] Abbreviations used: ATF4, activating transcription factor 4; *Cth*, cystathionine γ-lyase; eIF2, eukaryotic initiation factor 2; ER, endoplasmic reticulum; FGF21, fibroblast growth factor 21; GC, C57Bl/6J mice deleted for *Gcn2;* GCN2, general control nonderepressible 2; GSH, reduced glutathione; ISR, integrated stress response; MR, Met-restricted; Nrf2, nuclear factor-like 2; OD, obesogenic diet; p-eIF2, phosphorylated eukaryotic initiation factor 2; PERK, protein kinase R-like endoplasmic reticulum kinase; RER, respiratory exchange ratio; SCD, stearoyl-coenzyme A desaturase; WT, wild type; *Xbp1*, X-box–binding protein 1.

the experiment and then were provided with 8% deuterium-enriched drinking water until being killed (30–32).

Expt. 4. Young adult male and female mice aged 3–6 mo with a liver-specific deletion of PERK ($Perk^{flox/flox*AlbCre}$) and their Cre-negative littermates ($Perk^{flox/flox}$) (33) (n = 3–6 per strain and per diet, respectively) were conventionally housed as described previously and fed an OD or an MR diet for 5 wk.

In all studies, body weight and food intake were measured at regular intervals. At the end of each experiment, mice were killed by decapitation between 1400 and 1600. Mice tissues were rapidly dissected on ice, weighed, and flash-frozen in liquid nitrogen. Trunk blood was collected for serum. All samples were stored at −80°C until further processing.

Metabolic phenotyping. After 21 d on the experimental diet regimen, mice from Expt. 2 were placed into an Oxymax (Columbus Instruments) for 48 h. Metabolic and activity data were collected at 10-min intervals throughout the time in the chamber. The respiratory exchange ratio (RER) was calculated as a function of carbon dioxide production ($\dot{V}CO_2$) consumed to oxygen consumption ($\dot{V}O_2$) consumed, and energy expenditure was calculated as a function of VO_2 and lean body mass by the following formula:

$$[3.815 + (1.232 \times \text{RER} \times \text{VO}_2)] \times [\text{lean body mass (g)}] \times (1\ \text{L}/1000\ \text{mL}) \times (1\ \text{kg}/1000\ \text{g}) \quad (1)$$

Activity measures were taken for horizontal and vertical movements during the same time period. Body composition was measured with an MRI at regular intervals with the use of EchoMRI (Echo Medical Systems). Scans measured lean and fat masses and total and free water in each mouse. Canola oil was used for the initial systems testing.

Serum amino acids. Serum amino acids were analyzed with the use of HPLC as previously described (34).

Gene expression. Total RNA was extracted from frozen powdered liver with the use of TriReagent (Molecular Research Center) and a hand-held homogenizer. Samples were treated with DNase 1 (Life Technologies) after extraction and diluted into RNAsecure (Ambion). RNA quality (A260:A280) was measured with the use of a Nanodrop fluorospectrometer (Thermo Fisher Scientific). Complementary DNA was synthesized with the use of a high-capacity cDNA reverse transcription kit (Life Technologies) and then stored at −20°C. Real-time qPCR was conducted with the use of TaqMan Fast Universal PCR mastermix and specific TaqMan probes (Applied Biosystems) as previously described (35) (**Supplemental Table 1**). Amplification and detection were performed with the use of a StepOne real-time PCR system (Applied Biosystems). Samples were run in triplicate in 96-well plates, normalized to β-actin, and obtained with the use of the comparative C_T method [expressed with respect to the experimental control (WT OD)].

Protein extraction and immunoblotting. Frozen powdered liver was homogenized in an assay buffer [25 mM HEPES, 2 mM EDTA, 10 mM dithiothreitol, 50 mM sodium fluoride, 50 mM β-glycerophosphate pentahydrate, 3 mM benzamidine, 1 mM sodium orthovanadate, 0.5% sodium deoxycholate (Sigma-Aldrich), 1% SDS, protease inhibitor cocktail (Sigma-Aldrich), and 1 nM microcystin]. Equivalent amounts of protein

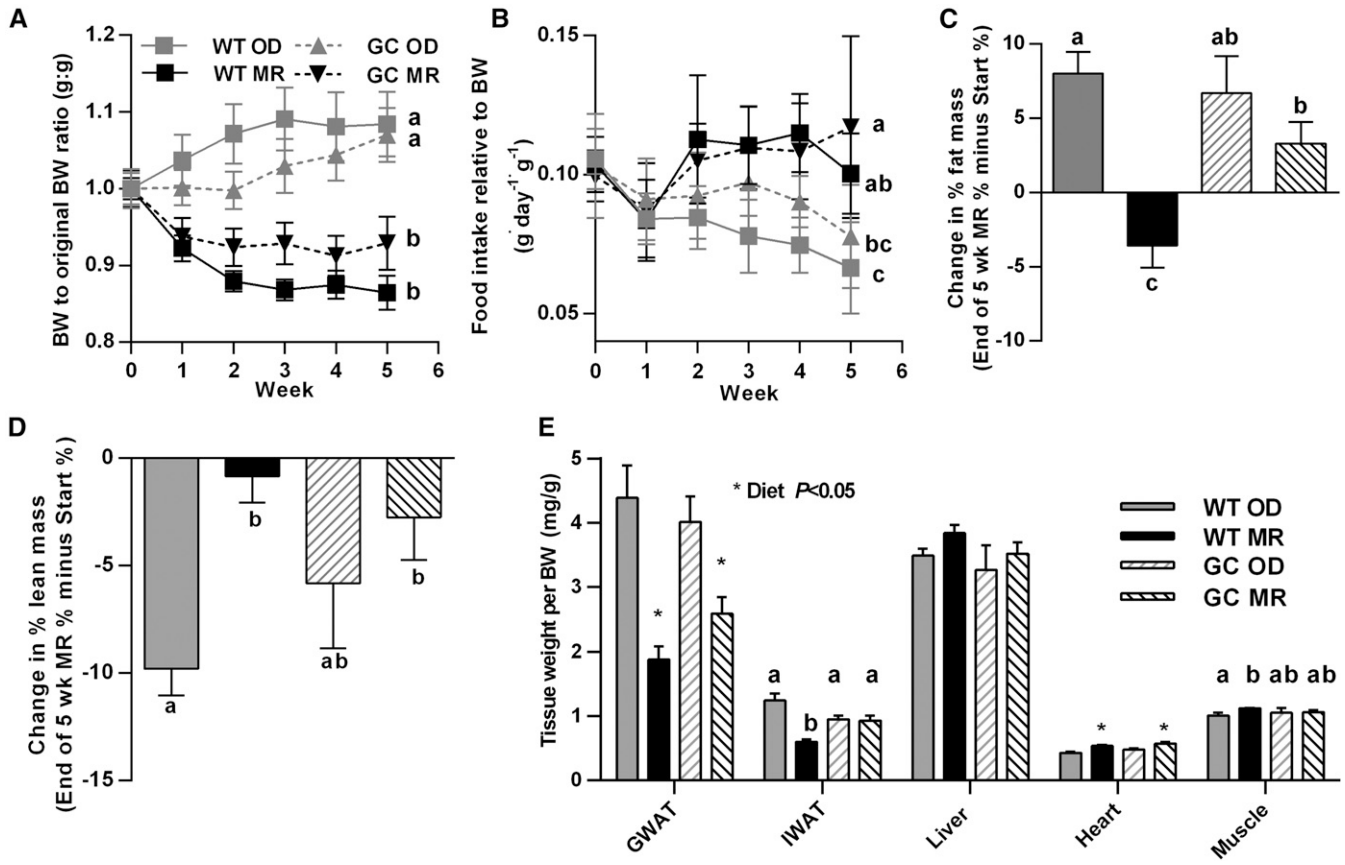

FIGURE 1 BW, body composition, and tissue weights in WT and GC mice fed an OD (0.86% Met) or an MR (0.12% Met) diet for 5 wk (Expt. 1). (A) Weekly BW change. (B) Weekly food intake. (C) Change in percentage of fat mass as measured by MRI. Values reflect the difference in body fat percentage (calculated as grams of fat mass per 100 g BW) between the start and end of the experiment. (D) Change in percentage lean mass as measured with the use of MRI. Values reflect the difference in lean mass percentage (calculated as grams of lean mass per 100 g BW) between the start and end of the experiment. (E) Final tissue weights adjusted for BW. Values are means ± SEMs (n = 6–8/group). Labeled means without a common lowercase letter differ, $P < 0.05$. BW, body weight; GC, C57Bl/6J mice deleted for general control nonderepressible 2; GWAT, gonadal white adipose tissue; IWAT, inguinal white adipose tissue; MR, Met-restricted; OD, obesogenic diet; WT, wild type.

from each sample were separated with the use of electrophoresis and transferred to polyvinylidene difluoride (Immobilon-P). Immunoblots were developed with the use of enhanced chemiluminesence (Amersham Biosciences) and imaged with the use of a FluroChem M imager (Protein Simple). Band densities were quantified with the use of Alphaview SA version 3.4.0 (Protein Simple). The p-eIF2 antibody was from Cell Signaling Technology, and the eIF2α used was from Santa Cruz Biotechnology.

Hepatic GSH assay. To measure intracellular concentrations of GSH, an OxisResearch-Bioxytech GSH/GSSG-412 assay kit was used as previously described (25). Briefly, pulverized frozen liver tissue was rinsed twice with ice-cold PBS and then centrifuged (100 × *g*; 10 min; 4°C). Samples were deproteinized with the use of 5% metaphosphoric acid in a 7:1 ratio with tissue weight. The resulting supernatants were diluted 1:60, and samples were run in a 96-well plate in triplicate.

eIF2B guanine nucleotide exchange factor activity assay. eIF2B activity was analyzed as previously described (36, 37). This protocol used the radioactivity of the binary complex eIF2[^{3}H]GDP and a liquid scintillation counter. The procedure was modified by purifying eIF2 from rabbit reticulocyte lysate from a crude eIF2 preparation (generously provided by William Merrick).

Protein synthesis measurements. At the start of experimental diets, a bolus dose of 99% enriched deuterium oxide was injected intraperitoneally to rapidly increase the body water pool to 5% enrichment (32, 38, 39). Mice were then freely provided drinking water enriched with 8% deuterium oxide throughout the time mice were fed the experimental diets. Two mice from each group were killed on days 1, 3, 7, 14, and 21 to determine new protein fraction in the gastrocnemius and liver. New protein fraction was determined by incorporating deuterium into proteins as measured by the enrichment of Ala as previously described (40, 41). From the changes in new protein fraction over time, the kinetic parameter *k* (1/*d*) was calculated with the use of a one-phase nonlinear curve fit. Protein synthesis was measured in the mixed (nuclei, plasma membranes, and myofibrillar components when analyzing skeletal muscle), cytosolic (all cytosolic organelles except mitochondria or nuclei), and mitochondrial subcellular fractions of both the liver and gastrocnemius.

Statistical analyses. All data are presented as means ± SEMs. Statistical analyses were completed with the use of Statistica version 8.0 (Statsoft Inc.). All data sets were tested for homogeneity of variance; if a data set failed, values were transformed by log base 10 and then retested for homogeneity. Conditions were compared with the use of 1- and 2-factor ANOVAs, with treatment group or mouse strain and diet as independent variables, respectively. When an overall ANOVA was significant ($P < 0.05$), differences between main factors or treatment groups were assessed with the use of Tukey's post hoc analysis ($P < 0.05$). Pearson correlations were conducted in Prism version 6 (GraphPad Software).

Results

Gcn2 status modulated body composition, feeding behavior, and energy expenditure to experimental diets. Experimental diets had no impact on body weight or composition at 2 d, but by 5 wk WT mice fed an OD gained ~10% body weight and ~8% body fat, reducing relative lean mass (**Figure 1**A, C, D). GC mice were initially resistant to weight gain by the OD, but by 5 wk body weight, body fat, and lean mass were not different from the WT OD group (Expt. 1). The MR diet increased food intake in WT and GC mice (Figure 1B), yet the mice became considerably leaner (Figure 1C–E) (Expt. 1). In

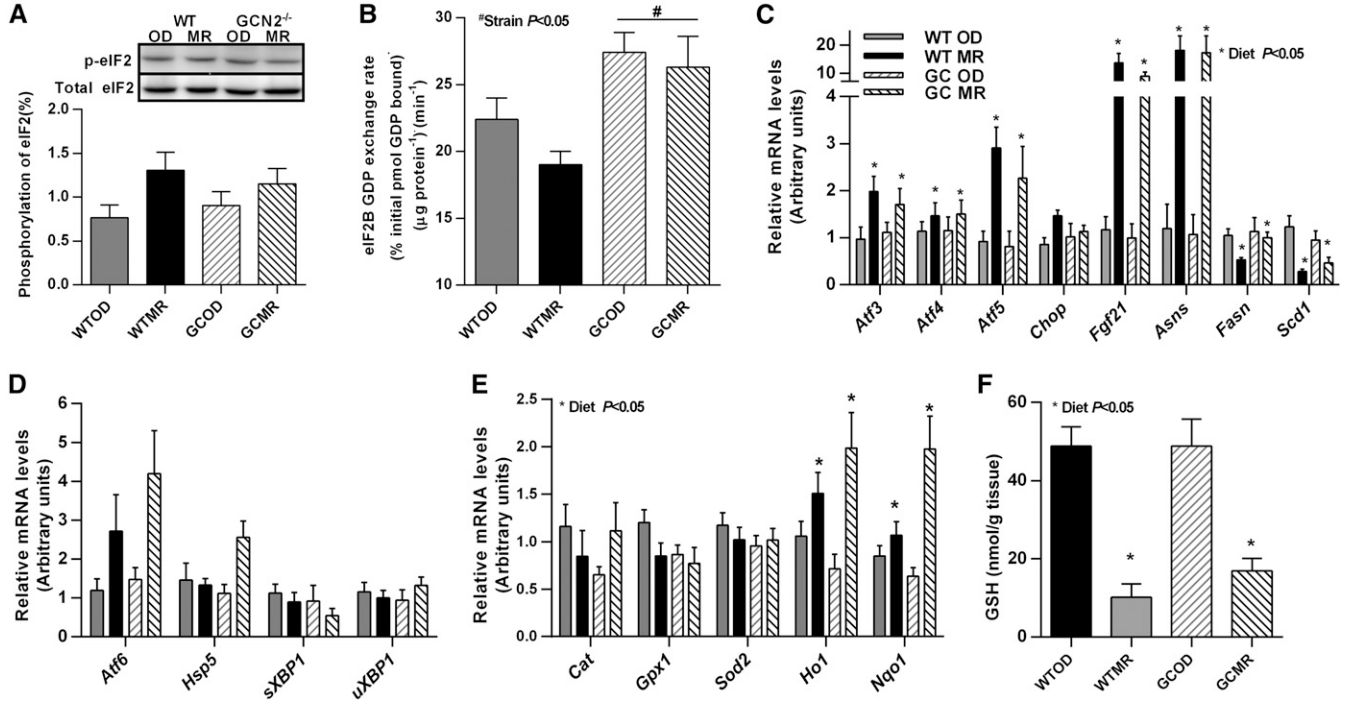

FIGURE 2 Biomarkers of the ISR and oxidative stress defenses in the livers of WT and GC mice fed an OD (0.86% Met) or an MR (0.12% Met) diet for 2 d (Expt. 1). (A) Phosphorylation of eIF2α at serine 51. (B) Guanine nucleotide exchange activity of eIF2B. (C) Genetic markers of the ISR. (D) Genetic markers of ER stress. (E) Antioxidant and NRF2-regulated genes. (F) GSH concentrations. Values are means ± SEMs (n = 6–8/group). *Asns*, asparagine synthetase; *Atf*, activating transcription factor; *Cat*, catalase; *Chop*, DNA damage-inducible transcript 3; eIF2α, eukaryotic initiation factor 2α; eIF2B, eukaryotic initiation factor 2B; ER, endoplasmic reticulum; *Fasn*, FA synthase; *Fgf21*, fibroblast growth factor 21; GC, C57Bl/6J mice deleted for *Gcn2*; GCN2, general control nonderepressible 2; *Gpx1*, glutathione peroxidase 1; GSH, glutathione; *Ho1*, heme oxygenase 1; *Hsp5*, heat-shock protein protease; ISR, integrated stress response; MR, Met-restricted; *Nqo1*, NAD(P)H quinone dehydrogenase 1; NRF2, nuclear factor-like 2; OD, obesogenic diet; *Scd1*, stearoyl-coenzyme A desaturase 1; *Sod2*, superoxide dismutase 2; *sXBP1*, spliced X-box–binding protein 1; *uXBP1*, unspliced X-box–binding protein 1; WT, wild type.

contrast, the MR diet did not substantially reduce body fat or improve relative measures of lean mass in GC mice.

In a separate study wherein mice were acclimated to wire-bottomed cages to control for coprophagia, GC mice fed an MR diet demonstrated increased vertical movement (**Supplemental Table 2**) accompanied by greater food spillage over time (**Supplemental Figure 1**A), suggesting foraging behavior (Expt. 2). Metabolic phenotyping conducted at 3 wk showed that the MR diet increased the RER in both WT and GC mice during the dark period (Supplemental Table 1). The MR diet also increased oxygen consumption and CO_2 production (independent effect of diet, $P < 0.05$; no strain difference), but these measures were reduced in GC mice compared with WT mice (independent effect of strain, $P < 0.05$), resulting in increased energy expenditure in WT but not GC mice fed an MR diet (Supplemental Figure 1E and Supplemental Table 1) (Expt. 3). This difference in energy expenditure corresponded with changes in body composition and tissue mass at 5 wk such that WT mice were measurably leaner than GC mice, although the MR diet reduced body weight in both WT and GC mice (Supplemental Figure 1B–E, G) (Expt. 3). These data show that GC mice were metabolically delayed in their response to the MR diet, suggesting that GCN2 influences early changes in body composition to an OD and MR diet.

MET restriction activated the ISR pathway independent of eIF2 phosphorylation. At 2 d, hepatic p-eIF2 was not altered by diet or strain (**Figure 2**A) (Expt. 1). GC mice displayed elevated eIF2B activity compared with WT mice (main effect of strain, $P < 0.05$), whereas the MR diet slightly reduced eIF2B activity in WT but not GC mice (Figure 2B). Nevertheless, mRNA expression of *Atf4* and the ATF4 target genes *Atf3*, *Atf5*, *Fgf21*, and asparagine synthetase (*Asns*) were increased, whereas stearoyl-coenzyme A desaturase 1 (*Scd1*), which encodes SCD1, was decreased by the MR diet in both WT and GC mice (Figure 2C). Genetic markers of ER stress were unchanged at 2 d (Figure 2D).

At 5 wk, liver p-eIF2 was increased by the MR diet in WT but not GC mice (**Figure 3**A) (Expt. 1). In contrast, hepatic eIF2B activity was decreased in both WT and GC mice fed the MR diet compared with the OD (Figure 3B), and ISR-regulated genes were substantially elevated in both WT and GC mice (**Figure 4**A). Specifically, hepatic *Atf4* mRNA was highest in GC mice, and *Fgf21* and *Asns* demonstrated ≥50-fold increases in mRNA abundance in both WT and GC mice. Genetic markers of FA oxidation [acyl-coenzyme A dehydrogenase, C-4 to C-12 straight chain (*Acadm*), and peroxisome proliferator-activated receptor γ 1 (*Pparg1*)] were increased in both WT and GC mice, whereas a genetic marker of FA synthesis [FA synthase (*Fasn*)] was not altered per diet or strain (Figure 4B). In contrast, *Scd1*, a genetic biomarker of lipogenesis, was decreased in WT but not GC mice. Furthermore, *Scd1* expression at 5 wk positively correlated with percentage body fat ($r = 0.73$; $P = 0.00001$) and combined fat pad weights ($r = 0.69$; $P = 0.00005$) (Expt. 1).

Finally, to assess whether the amplification of the hepatic ISR by the MR diet at 5 wk also reflected ER stress, we examined the mRNA expression of ER resident transcription factors activating transcription factor 6 (*Atf6*) and X-box–binding protein 1 (*Xbp1*) (unspliced and spliced forms) and the ER chaperone heat-shock protein family A member 5 (*Hspa5*; encoding BiP/Grp78) (Figure 4C) (Expt. 1). *Atf6* and unspliced *Xbp1* mRNA levels were slightly elevated in WT and GC mice (main effect of diet, $P < 0.05$), but spliced *Xbp1* was reduced in both WT and GC mice. In contrast, *Hspa5* mRNA expression was significantly

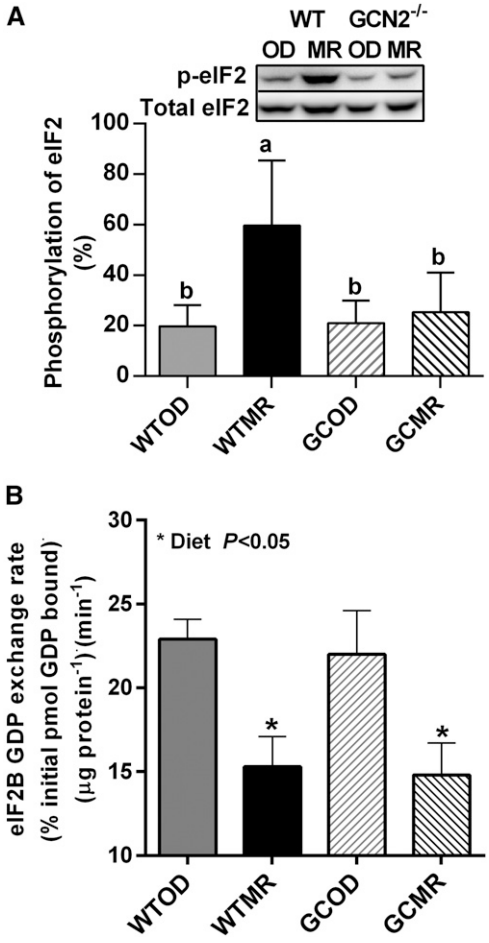

FIGURE 3 Biomarkers of the integrated stress response in the livers of WT and GC mice fed an OD (0.86% Met) or an MR (0.12% Met) diet for 5 wk (Expt. 1). (A) Phosphorylation of eIF2α at serine 51. (B) Guanine nucleotide exchange activity of eIF2B. Values are means ± SEMs (n = 6–8/group). Labeled means without a common lowercase letter differ, $P < 0.05$. eIF2, eukaryotic initiation factor 2; GC, C57Bl/6J mice deleted for *Gcn2*; GCN2, general control nonderepressible 2; MR, Met-restricted; OD, obesogenic diet; p-eIF2, phosphorylated eukaryotic initiation factor 2; WT, wild type.

increased in GC mice only (Expt. 1). These findings prompted us to examine PERK phosphorylation reflecting activation. Consistent with no increased p-eIF2 in GC mice, PERK phosphorylation was not increased by diet or strain (data not shown). Furthermore, $Perk^{flox/flox*AlbCre}$ mice were fed the MR diet for 5 wk and showed reduced body weight, leanness, and increased food intake and hepatic p-eIF2 similar to $Perk^{flox/flox}$ littermates (main effect of diet for all measurements) (**Supplemental Figure 2**A–E) (Expt. 4). Thus, the hepatic loss of PERK did not alter p-eIF2 or body composition as a result of the MR diet.

Met restriction altered the NRF2 oxidative stress response, transsulfuration pathway, and GSH independent of GCN2. At 2 d, the NRF2-regulated genes heme oxygenase 1 (*Ho1*) and NAD(P)H quinone dehydrogenase 1 (*Nqo1*) were increased by the MR diet in both WT and GC mice, whereas other antioxidant genes [catalase (*Cat*), *Gpx1*, and superoxide dismutase 2 (*Sod2*)] were unchanged (Figure 2E) (Expt. 1). Hepatic GSH concentrations were similarly reduced by the MR diet in both WT and GC mice (Figure 2F).

At 5 wk, NRF2-regulated genes *Ho1* and *Nqo1* were further increased by the MR diet in the livers of both WT and GC (Figure 4D)

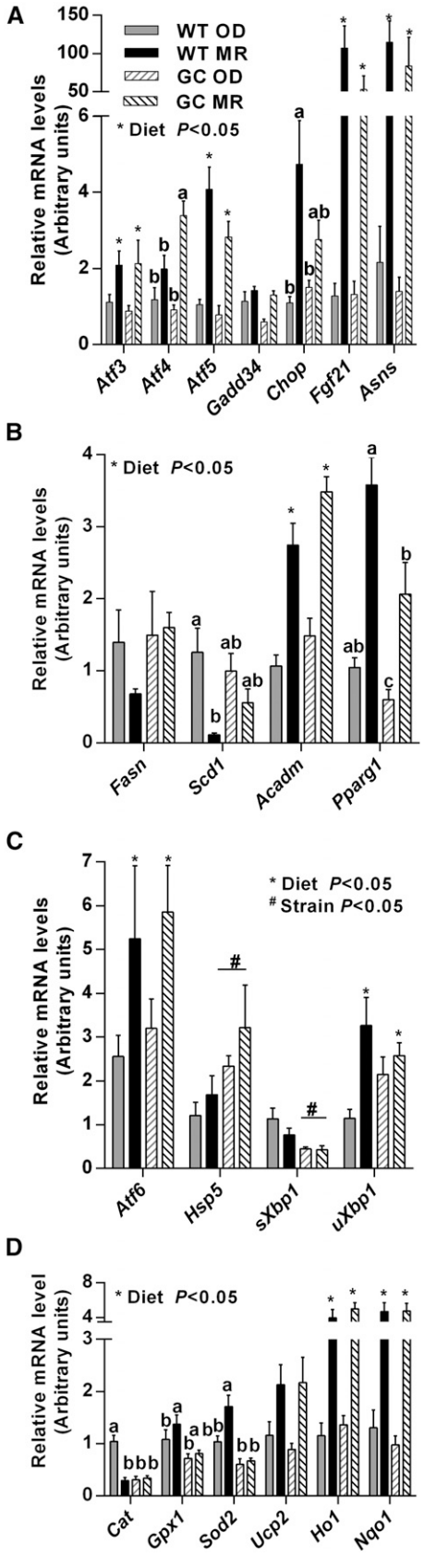

FIGURE 4 Transcript levels of genes representing the ISR, lipid metabolism, ER stress, and oxidative defenses in the liver of WT and *Gcn2*$^{-/-}$ (GC) mice fed an OD (0.86% Met) or an MR (0.12% Met) diet for 5 wk (Expt. 1). (A) Genetic markers of the ISR. (B) Genetic markers of lipid metabolism. (C) Genetic markers of ER stress. (D) Antioxidant and NRF2-regulated genes. Values are means ± SEMs (n = 6–8/group). Labeled means without a common lowercase letter differ, $P < 0.05$.

(Expt. 1). Other antioxidant genes (*Cat1*, *Gpx1*, and *Sod2*) showed variable responses in the livers of WT mice but uniformly low expression in the livers of GC mice.

An assessment of serum amino acids at 2 d and 5 wk showed that changes in response to the MR diet were relatively rapid and sustained (**Supplemental Table 3**) (Expt. 1). Specifically, the MR diet reduced circulating concentrations of Met and increased serum Ser, Thr, Gly, Ala, and Gln in both WT and GC mice, albeit the changes in Ser, Gly, and Ala were delayed in GC mice. Based on these amino acid patterns, we investigated the expression of genes that regulate the transsulfuration pathway. At 5 wk, the MR diet increased the hepatic expression of cystathionine γ-lyase (*Cth*), cystathionine β-synthase (*Cbs*), and 5-methyltetrahydrofolate-homocysteine methyltransferase (*Mtr*) transcripts in both WT and GC mice (**Figure 5**A). However, *Cth*, an ATF4-regulated gene, was reduced in the livers of GC mice fed the OD to 30% of WT mice fed the OD and only modestly increased in response to feeding an MR diet to 60% of WT mice fed the OD. Despite a higher expression of *Cth* in WT compared with GC mice fed the MR diet, liver GSH concentrations in WT and GC mice were similarly reduced to <25% of their own OD controls at 5 wk (Supplemental Figure 1F, Figure 5B) (Expt. 1).

Met restriction modulated liver and skeletal muscle protein synthesis rates independent of GCN2. The deuterium enrichment of Ala in proteins was measured over this time period to calculate protein synthesis rates (k) in the liver and skeletal muscle (gastrocnemius) (**Figure 6**) (Expt. 3). Independent of strain and in agreement with eIF2B activity at 5 wk, the MR diet substantially reduced the protein synthesis rates of cytosolic and mixed fractions in the liver and skeletal muscle, indicating a global suppression of protein synthesis rates. Interestingly, protein synthesis rates of the mitochondrial fraction were maintained in both the liver and skeletal muscle, indicating a differential regulation of mitochondrial proteins.

Discussion

In this study, the activation of the ATF4-driven ISR by dietary Met restriction did not correspond with eIF2 phosphorylation. Furthermore, p-eIF2 did not predict eIF2B activity or protein synthesis in mice fed the MR diet. These findings indicate that the long-term control of protein balance by restricting Met involves overlapping mechanisms of translational control that may include but do not require nutrient sensing by GCN2 or PERK. Furthermore, the activation of the ISR via ATF4 can occur absent substantial reductions in guanine nucleotide exchange on eIF2B,

Acadm, acyl-coenzyme A dehydrogenase, C-4 to C-12 straight chain; *Asns*, asparagine synthetase; *Atf*, activating transcription factor; *Cat*, catalase; *Chop*, DNA damage-inducible transcript 3; ER, endoplasmic reticulum; *Fasn*, FA synthase; *Fgf21*, fibroblast growth factor 21; *Gadd34*, growth arrest and DNA damage-inducible protein 34; GC, C57Bl/6J mice deleted for *Gcn2*; *Gcn2*, general control nonderepressible 2; *Gpx1*, glutathione peroxidase 1; *Ho1*, heme oxygenase 1; *Hsp5*, heat-shock protein protease; ISR, integrated stress response; MR, Met-restricted; *Nqo1*, NAD(P)H quinone dehydrogenase 1; NRF2, nuclear factor-like 2; OD, obesogenic diet; *Pparg1*, peroxisome proliferator-activated receptor γ 1; *Scd1*, stearoyl-coenzyme A desaturase 1; *Sod2*, superoxide dismutase 2; *sXbp1*, spliced X-box–binding protein 1; *Ucp2*, uncoupling protein 2; *uXbp1*, unspliced X-box–binding protein 1; WT, wild type.

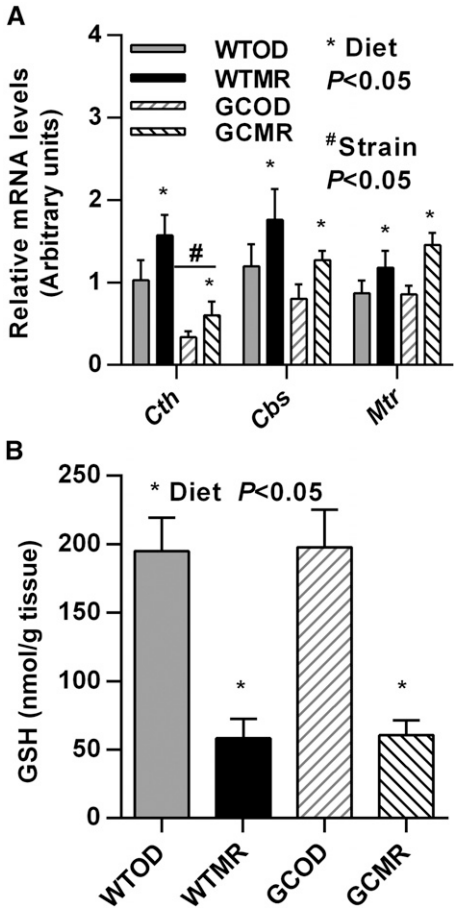

FIGURE 5 Transsulfuration pathway gene transcript levels and GSH concentrations in the liver of WT and *Gcn2*$^{-/-}$ (GC) mice fed an OD (0.86% Met) or an MR (0.12% Met) diet for 5 wk (Expt. 1). (A) Genes encoding components of the transsulfuration pathway. (B) GSH concentrations. Values are means ± SEMs (n = 6–8/group). *Cbs*, cystathionine β-synthase; *Cth*, cystathionine γ-lyase; GC, C57Bl/6J mice deleted for *Gcn2*; *Gcn2*, general control nonderepressible 2; GSH, glutathione; MR, Met-restricted; *Mtr*, 5-methyltetrahydrofolate-homocysteine methyltransferase; OD, obesogenic diet; WT, wild type.

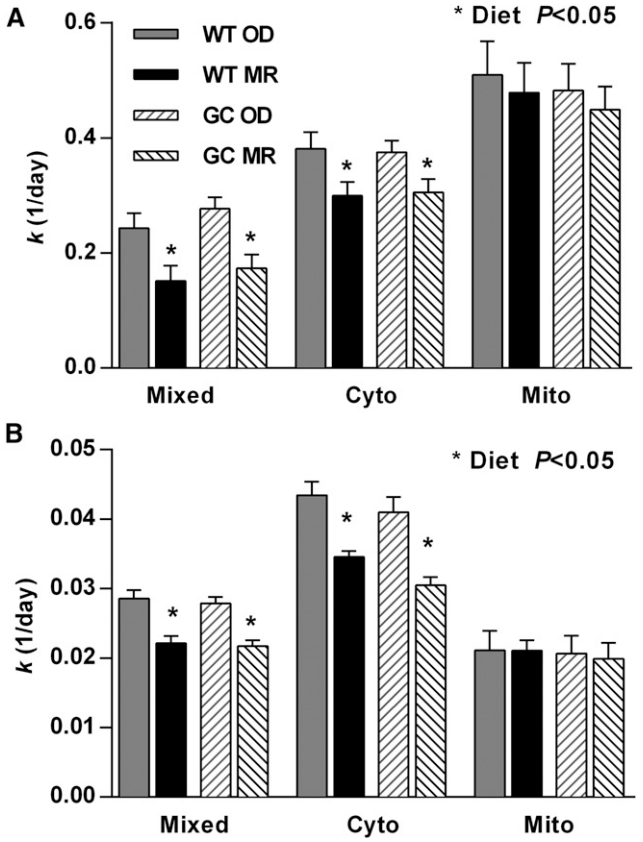

FIGURE 6 Protein synthesis rates (k) in subcellular fractions of the liver and skeletal muscle in WT and *Gcn2*$^{-/-}$ (GC) mice fed an OD (0.86% Met) or an MR (0.12% Met) diet for 21 d (Expt. 3). Mice were freely provided 8% deuterium-enriched drinking water after a bolus injection of 99% deuterium oxide at the start of the experiment. (A) Mixed, Cyto, and Mito fractions in the liver; (B) mixed, Cyto, and Mito fractions in skeletal muscle. Values are means ± SEMs (n = 10/group). Cyto, cytoplasmic; GC, C57Bl/6J mice deleted for *Gcn2*; *Gcn2*, general control nonderepressible 2; Mito, mitochondrial; MR, Met-restricted; OD, obesogenic diet; WT, wild type.

implicating other auxiliary means for increasing the expression of genes that are transcriptionally regulated by the ISR. Finally, in conjunction with reduced hepatic eIF2B activity from the MR diet, protein synthesis rates in mixed and cytosolic protein fractions, but not mitochondrial proteins, were reduced independent of p-eIF2 status. These findings extend our previous work that showed the MR activation of PERK by clarifying that p-eIF2 is not necessary for the activation of the ISR but that GCN2 does play a unique role in regulating body fat during Met restriction. Furthermore, these data challenge fundamental concepts about amino acid sensing and translational control and emphasize how the homeostatic response to amino acid stress in vivo is dynamic and influenced by time as well as the type and level of amino acid stress.

GCN2 played an early role in the physiologic alterations of energy expenditure and body composition to the MR diet. These outcomes agree with a recent study that showed that the loss of GCN2 delays but does not block the physiologic effects of dietary protein restriction (19). How GCN2 status influences body fat is suggested to involve the FGF21-directed regulation of lipid metabolism (42) but may also involve the regulation of lipogenesis via SCD1. The deletion of *Scd1* in mice promotes leanness and protects against diet-induced obesity (43), and variations in the human *SCD1* gene are associated with body fat distribution and insulin sensitivity (44, 45), leading to the idea that *Scd1* is a metabolic control point in body weight regulation (46). In agreement with this idea, we note herein that hepatic expression levels of *Scd1* positively correlated with percentage body fat and fat pad mass. Thus, the delayed fat loss in GC mice fed the MR diet may have been caused in part by altered *Scd1* expression in the liver and/or other tissues.

GSH, an antioxidant product of the transsulfuration pathway, decreases after sulfur amino acid deprivation or 50% dietary restriction (24, 47–50). Adding back Cys or the Cys donor *n*-acetylcysteine reverses this decrease (25), and this finding in combination with experiments in cultured HepG2 cells that have shown Cys to be the primary amino acid regulating cellular GSH homeostasis (51) suggests that the impact of Met restriction on GSH status may be attributed to Cys limitation. Studies in mice have shown that inhibiting GSH synthesis by a genetic defect or via buthionine sulfoximine results in a lean and insulin-sensitive phenotype (26, 27, 52, 53). How GSH depletion results in a lean phenotype is unclear. However, Met restriction

experiments in rats have suggested that Cys depletion alters lipogenesis via reduced SCD activity (54). The regulation of *Scd1* by ATF4 is well recognized, and ≥1 study has reported that *Atf4* deficiency in mice protects against the development of hepatic steatosis and obesity by high-fructose, high-fat diets via the suppression of SCD1 expression (55). Another study in liver cells showed that ATF4 deficiency reduces protein expression levels of SCD1 (56). Additional experiments are needed to further explore these relations and their influence on body fat and protein balance independent of p-eIF2 (57).

The transcriptional profile altered by Met insufficiency is distinct from other amino acids and reflects the activation of both an amino acid deprivation response and an NRF2-driven antioxidant response but not ER stress (58). Thus, it was unexpected to observe PERK phosphorylation in our previous study (25) and again to not observe it herein. However, considering that the data from this study indicate that the phosphorylation state of eIF2 is not a critical factor in the physiologic responses to Met restriction, we suggest that controlling ATF4 synthesis is the determining factor. This suggestion agrees with experiments in mouse embryonic fibroblasts that have shown that Met deprivation requires ATF4 and not eIF2 phosphorylation to alter mRNA levels of ISR-regulated genes (59). Studies have shown that in addition to translational control, ATF4 expression is subject to transcriptional regulation and alterations in protein stability (60, 61). How Met restriction promotes ATF4 expression is a future avenue to pursue. Furthermore, considering that ATF4 is a basic leucine zipper transcription factor that alters gene expression via dimerizing with other transcription factors such as NRF2, the relation of ATF4 with other nuclear factors is important to understand more fully.

The canonical hypothesis with respect to the translational control of protein synthesis by amino acid insufficiency involves reduced guanine nucleotide exchange on eIF2 via the phosphorylation of eIF2 by GCN2 (11, 14, 62). The loss of GCN2 function is thought to unleash control at this step, leading to a derepression of general protein synthesis during amino acid insufficiency. The inverse relation between p-eIF2 and eIF2B activity (and thus general protein synthesis) was originally established in cells in culture (62) and then supported by in vivo models of extreme amino acid deprivation or depletion/removal (12). Very few if any studies, to our knowledge, have examined translational control in tissues of animals fed diets restricted—not deprived of—one or more amino acids. This study shows that Met restriction represents a different kind of physiologic stress, one that may not alter tRNA charging but does alter eIF2B activity. The mechanism by which this occurs is unknown to our knowledge but may involve *1*) the regulation of eIF2B via a protein-protein interaction (63), *2*) the modification of eIF2B itself, *3*) the modulation of eIF5, the GTPase-activating protein in the nucleotide exchange reaction (64), or *4*) perhaps via a different type of modification on eIF2 such as deacetylation of the α subunit (65). In addition, the sensing of amino acid sufficiency via the mammalian target of rapamycin complex 1 may contribute to guiding protein synthesis to Met restriction. Future studies are needed to explore and reconcile these possibilities.

Consistent with reduced eIF2B activity during Met restriction, there was a global suppression of protein synthesis in both the liver and skeletal muscle independent of mouse strain. Interestingly, protein synthesis rates were maintained in the mitochondrial fractions of both strains during Met restriction despite global suppression of mixed and cytosolic fractions. This observation is consistent with rapamycin treatment (31), which inhibits the mechanistic target of rapamycin upstream of eIF2B. This selective synthesis of mitochondrial proteins during global protein synthesis suppression may represent a shared mechanism by which lifespan-extending approaches elicit beneficial physiologic responses.

In summary, this study identifies whole-body *Gcn2* status as playing a role in modulating body fat but not protein balance during Met restriction. Our findings further suggest that *Scd1* may contribute to GCN2-directed regulation of body fat in mice fed an MR diet. We show that activation of the ISR by restricting Met is uncoupled from p-eIF2, indicating that Met restriction activates overlapping mechanisms of translational control. These findings are further supported by the observation that restricting Met reduces protein synthesis in mixed and cytosolic fractions but not mitochondrial fractions in the liver and skeletal muscle. This study reveals the complexity of responses to MR diets and shows that the organismal response is dynamic over time.

Acknowledgments

We thank Cora Kerber, Lydia Kutzler and Berish B Wetstein for expert technical assistance. The authors' responsibilities were as follows—RCW and TGA: designed the research; APP, WOJ, ARB, ETM, FFP, YW, BFM, and KLH: conducted the research; APP, ARB, SRK, BFM, KLH, and TGA: analyzed the data; APP and TGA: wrote the manuscript; APP, WOJ, TWG, SRK, BFM, KLH, RCW, and TGA: edited the manuscript; TGA: had primary responsibility for the final content; and all authors: read and approved the final manuscript.

References

1. Orentreich N, Matias JR, DeFelice A, Zimmerman JA. Low methionine ingestion by rats extends life span. J Nutr 1993;123:269–74.
2. Edwards C, Canfield J, Copes N, Brito A, Rehan M, Lipps D, Brunquell J, Westerheide SD, Bradshaw PC. Mechanisms of amino acid-mediated lifespan extension in Caenorhabditis elegans. BMC Genet 2015;16:8.
3. Johnson JE, Johnson FB. Methionine restriction activates the retrograde response and confers both stress tolerance and lifespan extension to yeast, mouse and human cells. PLoS One 2014;9:e97729.
4. Lee BC, Kaya A, Ma S, Kim G, Gerashchenko MV, Yim SH, Hu Z, Harshman LG, Gladyshev VN. Methionine restriction extends lifespan of Drosophila melanogaster under conditions of low amino-acid status. Nat Commun 2014;5:3592.
5. Malloy VL, Krajcik RA, Bailey SJ, Hristopoulos G, Plummer JD, Orentreich N. Methionine restriction decreases visceral fat mass and preserves insulin action in aging male Fischer 344 rats independent of energy restriction. Aging Cell 2006;5:305–14.
6. Stone KP, Wanders D, Orgeron M, Cortez CC, Gettys TW. Mechanisms of increased in vivo insulin sensitivity by dietary methionine restriction in mice. Diabetes 2014;63:3721–33.
7. Malloy VL, Perrone CE, Mattocks DA, Ables GP, Caliendo NS, Orentreich DS, Orentreich N. Methionine restriction prevents the progression of hepatic steatosis in leptin-deficient obese mice. Metabolism 2013;62:1651–61.
8. Hasek BE, Boudreau A, Shin J, Feng D, Hulver M, Van NT, Laque A, Stewart LK, Stone KP, Wanders D, et al. Remodeling the integration of lipid metabolism between liver and adipose tissue by dietary methionine restriction in rats. Diabetes 2013;62:3362–72.
9. Miller RA, Buehner G, Chang Y, Harper JM, Sigler R, Smith-Wheelock M. Methionine-deficient diet extends mouse lifespan, slows immune and lens aging, alters glucose, T4, IGF-I and insulin levels, and increases hepatocyte MIF levels and stress resistance. Aging Cell 2005;4:119–25.

10. Anthony TG, Morrison CD, Gettys TW. Remodeling of lipid metabolism by dietary restriction of essential amino acids. Diabetes 2013;62:2635–44.
11. Zhang P, McGrath BC, Reinert J, Olsen DS, Lei L, Gill S, Wek SA, Vattem KM, Wek RC, Kimball SR, et al. The GCN2 eIF2alpha kinase is required for adaptation to amino acid deprivation in mice. Mol Cell Biol 2002;22:6681–8.
12. Anthony TG, McDaniel BJ, Byerley RL, McGrath BC, Cavener DR, McNurlan MA, Wek RC. Preservation of liver protein synthesis during dietary leucine deprivation occurs at the expense of skeletal muscle mass in mice deleted for eIF2 kinase GCN2. J Biol Chem 2004;279:36553–61.
13. Harding HP, Novoa I, Zhang Y, Zeng H, Wek R, Schapira M, Ron D. Regulated translation initiation controls stress-induced gene expression in mammalian cells. Mol Cell 2000;6:1099–108.
14. Mohammad-Qureshi SS, Jennings MD, Pavitt GD. Clues to the mechanism of action of eIF2B, the guanine-nucleotide-exchange factor for translation initiation. Biochem Soc Trans 2008;36:658–64.
15. Vattem KM, Wek RC. Reinitiation involving upstream ORFs regulates ATF4 mRNA translation in mammalian cells. Proc Natl Acad Sci USA 2004;101:11269–74.
16. Wang C, Guo F. Effects of activating transcription factor 4 deficiency on carbohydrate and lipid metabolism in mammals. IUBMB Life 2012;64:226–30.
17. Kilberg MS, Shan J, Su N. ATF4-dependent transcription mediates signaling of amino acid limitation. Trends Endocrinol Metab 2009;20:436–43.
18. Wilson GJ, Lennox BA, She P, Mirek ET, Al Baghdadi RJ, Fusakio ME, Dixon JL, Henderson GC, Wek RC, Anthony TG. GCN2 is required to increase fibroblast growth factor 21 and maintain hepatic triglyceride homeostasis during asparaginase treatment. Am J Physiol Endocrinol Metab 2015;308:E283–93.
19. Laeger T, Albarado DC, Burke SJ, Trosclair L, Hedgepeth JW, Berthoud HR, Gettys TW, Collier JJ, Munzberg H, Morrison CD. Metabolic responses to dietary protein restriction require an increase in FGF21 that is delayed by the absence of GCN2. Cell Reports 2016;16:707–16.
20. De Sousa-Coelho AL, Marrero PF, Haro D. Activating transcription factor 4-dependent induction of FGF21 during amino acid deprivation. Biochem J 2012;443:165–71.
21. Lee JI, Dominy JE Jr., Sikalidis AK, Hirschberger LL, Wang W, Stipanuk MH. HepG2/C3A cells respond to cysteine deprivation by induction of the amino acid deprivation/integrated stress response pathway. Physiol Genomics 2008;33:218–29.
22. Hayano M, Yang WS, Corn CK, Pagano NC, Stockwell BR. Loss of cysteinyl-tRNA synthetase (CARS) induces the transsulfuration pathway and inhibits ferroptosis induced by cystine deprivation. Cell Death Differ 2016;23:270–8.
23. Dickhout JG, Carlisle RE, Jerome DE, Mohammed-Ali Z, Jiang H, Yang G, Mani S, Garg SK, Banerjee R, Kaufman RJ, et al. Integrated stress response modulates cellular redox state via induction of cystathionine gamma-lyase: cross-talk between integrated stress response and thiol metabolism. J Biol Chem 2012;287:7603–14.
24. Sikalidis AK, Stipanuk MH. Growing rats respond to a sulfur amino acid-deficient diet by phosphorylation of the alpha subunit of eukaryotic initiation factor 2 heterotrimeric complex and induction of adaptive components of the integrated stress response. J Nutr 2010;140:1080–5.
25. Wanders D, Stone KP, Forney LA, Cortez CC, Dille KN, Simon J, Xu M, Hotard EC, Nikonorova IA, Pettit AP, et al. Role of GCN2-independent signaling through a non-canonical PERK/NRF2 pathway in the physiological responses to dietary methionine restriction. Diabetes 2016;65:1499–510.
26. Elshorbagy AK, Jerneren F, Scudamore CL, McMurray F, Cater H, Hough T, Cox R, Refsum H. Exploring the lean phenotype of glutathione-depleted mice: thiol, amino acid and fatty acid profiles. PLoS One 2016;11:e0163214.
27. Findeisen HM, Gizard F, Zhao Y, Qing H, Jones KL, Cohn D, Heywood EB, Bruemmer D. Glutathione depletion prevents diet-induced obesity and enhances insulin sensitivity. Obesity (Silver Spring) 2011;19:2429–32.
28. Report of the American Institute of Nutrition ad hoc Committee on Standards for Nutritional Studies. J Nutr 1977;107:1340–8.
29. Ables GP, Perrone CE, Orentreich D, Orentreich N. Methionine-restricted C57BL/6J mice are resistant to diet-induced obesity and insulin resistance but have low bone density. PLoS One 2012;7:e51357.
30. Drake JC, Bruns DR, Peelor FF III, Biela LM, Miller RA, Miller BF, Hamilton KL. Long-lived snell dwarf mice display increased proteostatic mechanisms that are not dependent on decreased mTORC1 activity. Aging Cell 2015;14:474–82.
31. Drake JC, Peelor FF III, Biela LM, Watkins MK, Miller RA, Hamilton KL, Miller BF. Assessment of mitochondrial biogenesis and mTORC1 signaling during chronic rapamycin feeding in male and female mice. J Gerontol A Biol Sci Med Sci 2013;68:1493–501.
32. Drake JC, Bruns DR, Peelor FF III, Biela LM, Miller RA, Hamilton KL, Miller BF. Long-lived crowded-litter mice have an age-dependent increase in protein synthesis to DNA synthesis ratio and mTORC1 substrate phosphorylation. Am J Physiol Endocrinol Metab 2014;307:E813–21.
33. Teske BF, Wek SA, Bunpo P, Cundiff JK, McClintick JN, Anthony TG, Wek RC. The eIF2 kinase PERK and the integrated stress response facilitate activation of ATF6 during endoplasmic reticulum stress. Mol Biol Cell 2011;22:4390–405.
34. Phillipson-Weiner L, Mirek ET, Wang Y, McAuliffe WG, Wek RC, Anthony TG. General control nonderepressible kinase 2 (GCN2) deletion predisposes to asparaginase-associated pancreatitis in mice. Am J Physiol Gastrointest Liver Physiol 2016;310:G1061–40.
35. Wilson GJ, Bunpo P, Cundiff JK, Wek RC, Anthony TG. The eukaryotic initiation factor 2 kinase GCN2 protects against hepatotoxicity during asparaginase treatment. Am J Physiol Endocrinol Metab 2013;305:E1124–33.
36. Kimball SR, Everson WV, Flaim KE, Jefferson LS. Initiation of protein synthesis in a cell-free system prepared from rat hepatocytes. Am J Physiol 1989;256:C28–34.
37. Woo CW, Kutzler L, Kimball SR, Tabas I. Toll-like receptor activation suppresses ER stress factor CHOP and translation inhibition through activation of eIF2B. Nat Cell Biol 2012;14:192–200.
38. Neese RA, Misell LM, Turner S, Chu A, Kim J, Cesar D, Hoh R, Antelo F, Strawford A, McCune JM, et al. Measurement in vivo of proliferation rates of slow turnover cells by 2H2O labeling of the deoxyribose moiety of DNA. Proc Natl Acad Sci USA 2002;99:15345–50.
39. Miller BF, Robinson MM, Bruss MD, Hellerstein M, Hamilton KL. A comprehensive assessment of mitochondrial protein synthesis and cellular proliferation with age and caloric restriction. Aging Cell 2012;11:150–61.
40. Miller BF, Drake JC, Naylor B, Price JC, Hamilton KL. The measurement of protein synthesis for assessing proteostasis in studies of slowed aging. Ageing Res Rev 2014;18:106–11.
41. Miller BF, Wolff CA, Peelor FF III, Shipman PD, Hamilton KL. Modeling the contribution of individual proteins to mixed skeletal muscle protein synthetic rates over increasing periods of label incorporation. J Appl Physiol(1985);2015:655–61.
42. Laeger T, Henagan TM, Albarado DC, Redman LM, Bray GA, Noland RC, Munzberg H, Hutson SM, Gettys TW, Schwartz MW, et al. FGF21 is an endocrine signal of protein restriction. J Clin Invest 2014;124:3913–22.
43. Ntambi JM, Miyazaki M, Stoehr JP, Lan H, Kendziorski CM, Yandell BS, Song Y, Cohen P, Friedman JM, Attie AD. Loss of stearoyl-CoA desaturase-1 function protects mice against adiposity. Proc Natl Acad Sci USA 2002;99:11482–6.
44. Warensjö E, Ingelsson E, Lundmark P, Lannfelt L, Syvanen AC, Vessby B, Riserus U. Polymorphisms in the SCD1 gene: associations with body fat distribution and insulin sensitivity. Obesity (Silver Spring) 2007;15:1732–40.
45. Martín-Núñez GM, Cabrera-Mulero R, Rojo-Martinez G, Gomez-Zumaquero JM, Chaves FJ, de Marco G, Soriguer F, Castano L, Morcillo S. Polymorphisms in the SCD1 gene are associated with indices of stearoyl CoA desaturase activity and obesity: a prospective study. Mol Nutr Food Res 2013;57:2177–84.
46. Dobrzyn A, Ntambi JM. The role of stearoyl-CoA desaturase in body weight regulation. Trends Cardiovasc Med 2004;14:77–81.
47. Dobrzyn P, Dobrzyn A, Miyazaki M, Cohen P, Asilmaz E, Hardie DG, Friedman JM, Ntambi JM. Stearoyl-CoA desaturase 1 deficiency increases fatty acid oxidation by activating AMP-activated protein kinase in liver. Proc Natl Acad Sci USA 2004;101:6409–14.
48. Maddineni S, Nichenametla S, Sinha R, Wilson RP, Richie JP Jr. Methionine restriction affects oxidative stress and glutathione-related redox pathways in the rat. Exp Biol Med (Maywood) 2013;238:392–9.
49. Brown-Borg HM, Rakoczy S, Wonderlich JA, Armstrong V, Rojanathammanee L. Altered dietary methionine differentially impacts glutathione and methionine metabolism in long-living growth hormone-deficient Ames dwarf and wild-type mice. Longev Healthspan 2014;3:10.
50. Hine C, Harputlugil E, Zhang Y, Ruckenstuhl C, Lee BC, Brace L, Longchamp A, Trevino-Villarreal JH, Mejia P, Ozaki CK, et al. Endogenous hydrogen sulfide production is essential for dietary restriction benefits. Cell 2015;160:132–44.

51. Yu X, Long YC. Crosstalk between cystine and glutathione is critical for the regulation of amino acid signaling pathways and ferroptosis. Sci Rep 2016;6:30033.
52. Kendig EL, Chen Y, Krishan M, Johansson E, Schneider SN, Genter MB, Nebert DW, Shertzer HG. Lipid metabolism and body composition in Gclm(−/−) mice. Toxicol Appl Pharmacol 2011;257:338–48.
53. Haque JA, McMahan RS, Campbell JS, Shimizu-Albergine M, Wilson AM, Botta D, Bammler TK, Beyer RP, Montine TJ, Yeh MM, et al. Attenuated progression of diet-induced steatohepatitis in glutathione-deficient mice. Lab Invest 2010;90:1704–17.
54. Elshorbagy AK, Valdivia-Garcia M, Mattocks DA, Plummer JD, Smith AD, Drevon CA, Refsum H, Perrone CE. Cysteine supplementation reverses methionine restriction effects on rat adiposity: significance of stearoyl-coenzyme A desaturase. J Lipid Res 2011;52:104–12.
55. Li H, Meng Q, Xiao F, Chen S, Du Y, Yu J, Wang C, Guo F. ATF4 deficiency protects mice from high-carbohydrate-diet-induced liver steatosis. Biochem J 2011;438:283–9.
56. Ren LP, Yu X, Song GY, Zhang P, Sun LN, Chen SC, Hu ZJ, Zhang XM. Impact of activating transcription factor 4 signaling on lipogenesis in HepG2 cells. Mol Med Rep 2016;14:1649–58.
57. Guan BJ, Krokowski D, Majumder M, Schmotzer CL, Kimball SR, Merrick WC, Koromilas AE, Hatzoglou M. Translational control during endoplasmic reticulum stress beyond phosphorylation of the translation initiation factor eIF2alpha. J Biol Chem 2014;289:12593–611.
58. Chen H, Song R, Wang G, Ding Z, Yang C, Zhang J, Zeng Z, Rubio V, Wang L, Zu N, et al. OLA1 regulates protein synthesis and integrated stress response by inhibiting eIF2 ternary complex formation. Sci Rep 2015;5:13241.
59. Mazor KM, Stipanuk MH. GCN2- and eIF2alpha-phosphorylation-independent, but ATF4-dependent, induction of CARE-containing genes in methionine-deficient cells. Amino Acids 2016;48:2831–42.
60. Dey S, Baird TD, Zhou D, Palam LR, Spandau DF, Wek RC. Both transcriptional regulation and translational control of ATF4 are central to the integrated stress response. J Biol Chem 2010;285:33165–74.
61. Ehren JL, Maher P. Concurrent regulation of the transcription factors Nrf2 and ATF4 mediates the enhancement of glutathione levels by the flavonoid fisetin. Biochem Pharmacol 2013;85:1816–26.
62. Kimball SR. Regulation of translation initiation by amino acids in eukaryotic cells. Prog Mol Subcell Biol 2001;26:155–84.
63. Palmesino E, Apuzzo T, Thelen S, Mueller B, Langen H, Thelen M. Association of eukaryotic translation initiation factor eIF2B with fully solubilized CXCR4. J Leukoc Biol 2016;99:971–8.
64. Jennings MD, Pavitt GD. A new function and complexity for protein translation initiation factor eIF2B. Cell Cycle 2014;13:2660–5.
65. Prola A, Silva JP, Guilbert A, Lecru L, Piquereau J, Ribeiro M, Mateo P, Gressette M, Fortin D, Boursier C, et al. SIRT1 protects the heart from ER stress-induced cell death through eIF2alpha deacetylation. Cell Death Differ 2016;24:343–356.